Pergamon

Tetrahedron 57 (2001) 4115–4122

TETRAHEDRON

Further study of axial chirality due to an acyclic imide N–Ar bond: control of rotational barrier by electronic effects of acyl groups

Kazuhiro Kondo,[a] Takeko Iida,[a] Hiroko Fujita,[a] Tomoko Suzuki,[a] Ryoko Wakabayashi,[a] Kentaro Yamaguchi[b] and Yasuoki Murakami[a,*]

[a]*School of Pharmaceutical Sciences, Toho University, 2-2-1 Miyama, Funabashi, Chiba 274-8510, Japan*
[b]*Chemical Analysis Center, Chiba University, 1-33 Yayoi-cho, Inage-ku, Chiba 263-8522, Japan*

Received 15 February 2001; accepted 9 March 2001

Abstract—Studies on stability to racemization in a series of optically active *N*-aroyl-*N*-(2-*t*-butylphenyl)acetamides **2a–g** (X=NMe_2, OMe, Me, H, F,Cl, CF_3), depending on the electronic effect of their aroyl groups, are described. It has been revealed that the stability of **2** bearing stronger electron-withdrawing groups on the aroyl benzene ring was enhanced, with linear correlation between the $\Delta G^{\ddagger}$ and Hammett's σ_p *para*-substituent constant of **2a–g**. Furthermore, the absolute configuration of optically active imides **2a–g** has been determined by comparison with the CD spectrum of (*S*)-*N*-(2-*t*-butylphenyl)-*N*-(4-trifluoromethylbenzoyl)propionamide (**5b**) derived from (R_a,2*S*)-*N*-(2-*t*-butylphenyl)-*N*-(4-trifluoromethylbenzoyl)-2-acetoxypropionamide (**4b**), whose absolute configuration was determined by X-ray analysis.

1. Introduction

Recently, optically active non-biaryl compounds, which possess axial chirality based on an anilide N–Ar bond, have been utilized for stereoselective syntheses.[1,2] The key issue is considered to be the relationship between the rotation barrier around the N–Ar bonds and the disposition of substituents. However, few fundamental studies of these rotation barriers have been reported.[3] Quite recently, we have reported the first example of optically active imides **1** which possess axial chirality based on an acyclic imide N–Ar bond rotation.[4] Furthermore, in relation to the steric effects of acyl groups, we have revealed that **1** bearing a bulky acyl group rather than a relatively small one racemized more easily.[4] As part of our research program in relation to optically active N–Ar axially chiral compounds, we undertook investigation of the relationship between the stability to racemization and the electronic effects of acyl groups. In this paper, we describe our study on the stability to racemization in a series of optically active *N*-aroyl-*N*-(2-*t*-butylphenyl)acetamides **2a–g** bearing various *para*-substituents (X=NMe_2, OMe, Me, H, F, Cl, CF_3) on the aroyl benzene ring.[5]

2. Results and discussion

In order to effect a control system for N–Ar rotation barriers, namely, stability to racemization, based on electronic effects of acyl groups, optically active imides **2a–g** were selected as the test substrates (Fig. 1). At first, the stability to racemization in benzene at 40°C (sealed-tube experiments) was investigated with optically active imides **2a–g**, which were prepared by the aroylation of 2-*t*-butylphenylacetamide, and the subsequent optical resolution of racemic imides (±)-**2a–g** using semipreparative HPLC (Daicel Chiralcel OD, eluent: *i*-PrOH-hexane). The use of other solvents such as DMF and MeCN in place of benzene led to the decomposition of **2**. The rate constants *k* for their racemization are shown in Table 1. The stability to racemization was delicately controlled by the electronic effect of

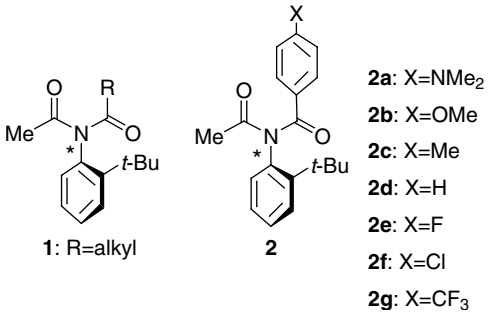

Figure 1.

Keywords: N–C axial chirality; electronic effect; acyclic imide; rotational barrier; Hammett's σ_p *para*-substituent constant.
* Corresponding author. Tel: +81-47-472-1585; fax +81-47-472-1595; e-mail: murakami@phar.toho-u.ac.jp

0040–4020/01/$ - see front matter © 2001 Elsevier Science Ltd. All rights reserved.
PII: S0040-4020(01)00295-2

Table 1. Configurational stability to racemization with optically active imides **2a–g** in benzene at 40°C

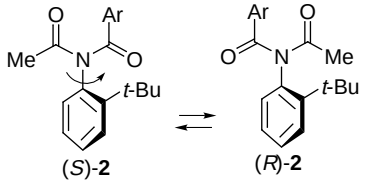

(*S*)-**2** (*R*)-**2**

Entry	Compound (X)	k [10^{-6}(S^{-1})]
1	**2a** (NMe_2)	9.08±0.02
2	**2b** (OMe)	4.26±0.37
3	**2c** (Me)	2.93±0.02
4	**2d** (H)	2.74±0.09
5	**2e** (F)	2.23±0.05
6	**2f** (Cl)	1.79±0.03
7	**2g** (CF_3)	1.33±0.27

Table 2. Transition-state functions of optically active imides **2a–g**

Entry	Compound (X=)	$\Delta H^{\ddagger a}$ (kcal/mol)	$\Delta S^{\ddagger a}$ (cal/K·mol)	$\Delta G^{\ddagger}$ at 27°C (kcal/mol)
1	**2a** (NMe_2)	22.6	−9.4	25.4
2	**2b** (OMe)	25.1	−2.8	25.9
3	**2c** (Me)	24.1	−7.0	26.2
4	**2d** (H)	25.0	−4.1	26.2
5	**2e** (F)	23.8	−8.4	26.3
6	**2f** (Cl)	26.0	−2.0	26.6
7	**2g** (CF_3)	28.2	4.8	26.8

[a] The transition-state functions were calculated according to the Eyring's equation.

the *para*-substituent on the aroyl benzene ring. As a result, it was found that the stability of **2** bearing stronger electron-withdrawing groups on the aroyl benzene ring was enhanced.

Next, measurement of the rate constants k for the racemization was performed with optically active imides **2a–g** in benzene at three other temperatures. By using these data, the transition-state functions for racemization were obtained from the Eyring equation as shown in Table 2.[6] The enthalpies of activation $\Delta H^{\ddagger}$ of **2a–g** were 22.6, 25.1, 24.1, 25.0, 23.8, 26.0 and 28.2 kcal/mol, respectively. The small value of the $\Delta H^{\ddagger}$ for **2a** (22.6) relative to **2g** (28.2) would be mainly due to the destabilization in the ground state. The entropies of activation $\Delta S^{\ddagger}$ for racemization of **2a–g** were from −9.4 to 4.8 cal/K.mol. The much smaller value of $\Delta S^{\ddagger}$ for **2a** (−9.4), **2c** (−7.0) and **2e** (−8.4) relative to **2g** (4.8) would be indicative of a more highly ordered transition state (relative to the ground state) for the former. The free energies of activation $\Delta G^{\ddagger}$ were changed by 1.4 kcal/mol from **2a** to **2g**. As shown in Fig. 2, linear correlation between the $\Delta G^{\ddagger}$ and Hammett's σ_p *para*-substituent constant[7] of **2a–g** was observed.

The structural distinction between the most unstable imide (±)-**2a** bearing an NMe_2 group and the most stable imide (±)-**2g** bearing a CF_3 group[4b] was confirmed by X-ray crystallographic analysis. The representative ORTEP drawing of **2a** is shown in Fig. 3. The 2-*t*-butylphenyl group and the imide plane of both **2a** and **2g** were approximately orthogonal, and their imide geometry was the *exo–endo* arrangement[8] with acetyl carbonyl *trans* and aroyl carbonyl *cis* to the 2-*t*-butylphenyl group. The nature of imide nitrogen can be represented in terms of two angle parameters, the summation of the three valence angles around the nitrogen θ, and the twist angle[9] τ of the amide bond calculated by the average of ω_1 ($C^3C^2NC^5$) and ω_2 ($O^2C^2NC^1$), its range[10] being between 0 and 90° (the highest τ value[11] reported for imide is 83.2°). The parameters of **2a** and **2g** are shown in Table 3. The essentially sp^2 nature of the imide nitrogen in **2g** was confirmed: θ=359.8° (the

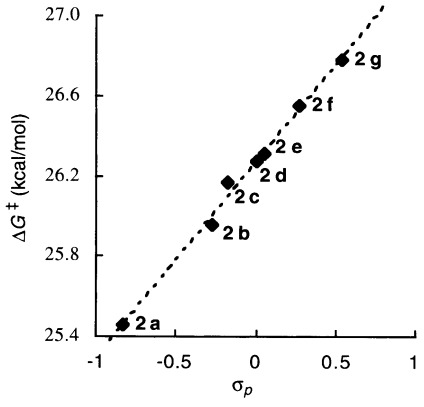

Figure 2. Plot of $\Delta G^{\ddagger}$ vs. σ_p for **2a–g**.

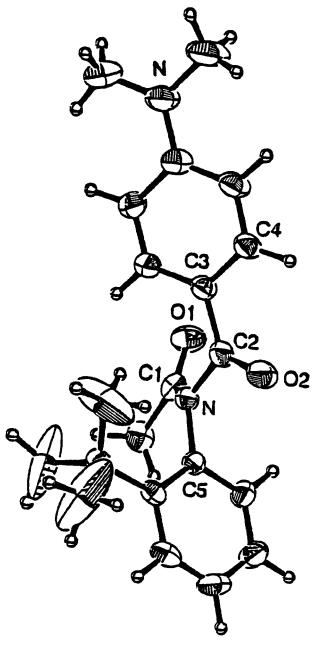

Figure 3. The ORTEP drawing of (±)-**2a**

Table 3. Angle around N, twist angle, and selected bond lengths of **2a** and **2g**

Entry	Compound (X=)	Angle around N θ (°)	Twist angle[a] τ of aroyl bond (°)	C^1–N Å	C^1=O^1 Å	C^2–N Å	C^2=O^2 Å	N–C^5 Å
1	**2a** (NMe_2)	352.8	31.6	1.422(6)	1.200(5)	1.435(6)	1.207(5)	1.455(5)
2	**2g** (CF_3)	359.8	18.5	1.432(10)	1.199(9)	1.374(10)	1.213(9)	1.477(9)

[a] The twist angle τ was calculated by the average of $\omega_1(C^3C^2NC^5)$ and $\omega_2(O^2C^2NC^1)$.

angle θ of the ideal sp^2 planar nitrogen atom is 360°). On the other hand, the angle θ of **2a** indicated a small pyramidalization of the imide nitrogen: 352.8° (the angle θ of the ideal sp^3 nitrogen atom is 328.4°). The twist angle τ of **2a** was larger than that of **2g** (**2a**: 31.6°, **2g**: 18.5°). The aroyl C(O)–N bond of **2a** (1.435 (6) Å was elongated as compared with that of **2g** (1.374 (10) Å, although no marked change in the length of other acetyl C(O)–N, C=O and N–Ar bonds was observed.[12] Taking all the experimental results into consideration, one possible mechanism for the more facile racemization of **2a** compared with **2g**, would be as follows. A possible transition state for the racemization is considered to be two modes (Fig. 4), which are the transition state **2-A** wherein the aroyl carbonyl group is close to the *t*-butyl group and the transition state **2-B** wherein the acetyl methyl group is, but molecular modeling studies suggested that the transition state **2-A** seemed to be more favored than the transition state **2-B**. Therefore, the weaker aroyl C(O)–N double bond character of **2a**, compared with **2g**, causes a decrease of the steric repulsion between the aroyl carbonyl and the 2-*t*-butyl group in **2-A**, facilitating the N–Ar bond rotation of **2a**. Additionally, due to the nitrogen pyramidalization and the imide twist in **2a**, **2a** is more destabilized in the ground state than **2g**. And so the activation energy of **2a** for racemization is smaller than that of **2g**. Thus, the racemization of **2a** is more facile than that of **2g**. The possibility that the change in the N–Ar rotational barrier originates in the double bond character of the N–Ar single bond was also considered. However, from the X-ray

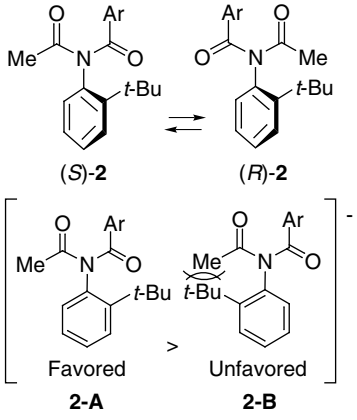

Figure 4.

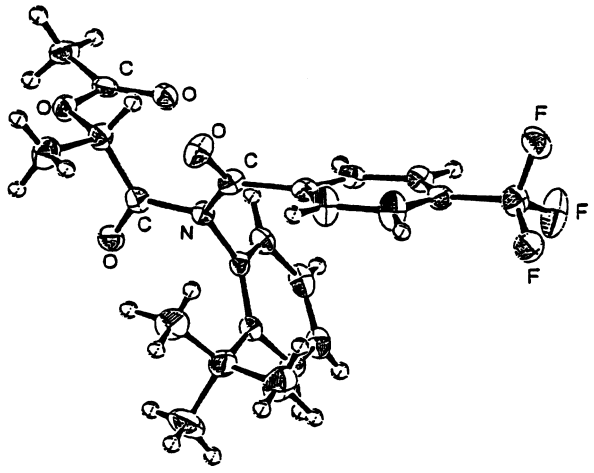

Figure 5. The ORTEP drawing of **4b**.

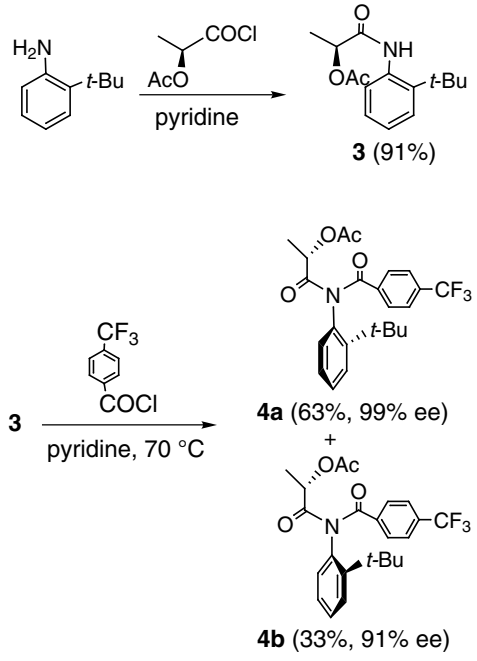

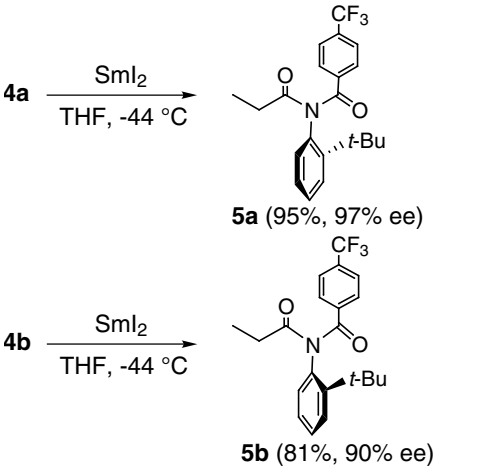

Scheme 1.

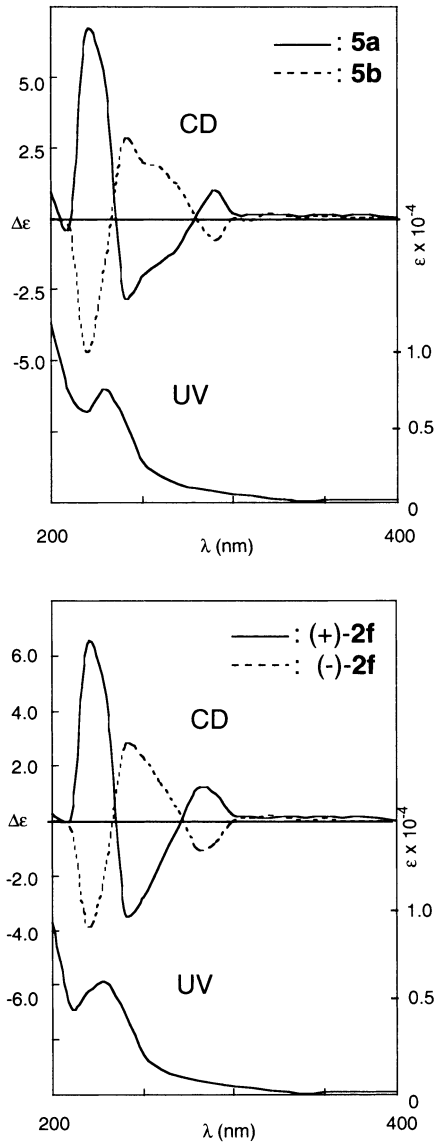

Figure 6. The representative CD and UV spectra of **5a**, **5b**, (+)-**2f** and (−)-**2f** in CH_3CN.

analyses of **2a** and **2g** (Table 3), there was no marked change in the length of the N–Ar single bond.

The assignment of the absolute configurations of optically active imides **2a–g** was established by comparison with the CD spectrum of **5b** derived from **4a**,[13,14] whose absolute configuration was determined by X-ray analysis (Fig. 5). The preparation of **4a** and **4b** is shown in Scheme 1. Acylation of 2-*t*-butylaniline with (*S*)-2-acetoxypropionyl chloride in pyridine and further aroylation (4-trifluoromethylbenzoyl chloride in pyridine) afforded the separable diastereomers **4a** with 99% ee and **4b** with 91% ee as a ca. 2:1 mixture. Treatment of the separated diastereomers **4a** and **4b** with SmI_2 in THF at −44°C afforded **5a** and **5b** with 97 and 90% ee, respectively.[15] The representative CD spectra of **5a,b** and **2f** are shown in Fig. 6. Thus, the absolute configurations of **2a,b** with positive values of the specific rotation and **2c–g** with negative values of the specific rotation, were determined to be *S* as shown in Fig. 7.

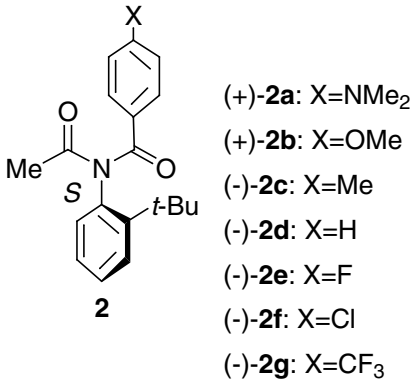

Figure 7. The absolute configurations of (+)-**2a,b** and (−)-**2c–g**.

3. Conclusion

We have demonstrated that the stability to racemization of **2** bearing stronger electron-withdrawing groups on the aroyl benzene ring is enhanced, with linear correlation between the $\Delta G^{\ddagger}$ and Hammett's σ_p *para*-substituent constant of **2a–g**. Furthermore, the absolute configurations of **2a,b** with positive values of the specific rotation and **2c–g** with negative values of the specific rotation were determined to be *S*. Further studies along this line are in progress.

4. Experimental

4.1. General

All melting points (mp) were determined on a Yanagimoto melting point apparatus and are uncorrected. IR spectra were measured on a JASCO FT/IR-230 diffraction grating IR spectrophotometer. ^1H and ^{13}C NMR spectra were measured on a JEOL AL-400 or EX-400 NMR spectrometer, operating at 400 MHz for ^1H NMR and at 100 MHz at ^{13}C NMR. ^1H and ^{13}C NMR spectra were reported in δ units, parts per million (ppm) downfield from tetramethylsilane (δ=0). EI MS spectra were measured on a JEOL JMS-DX-303 instrument. Specific rotations (in deg cm^3 g^{-1} L^{-1}) were determined on a JASCO DIP-1000 digital polarimeter. UV spectra were measured on a Shimadzu UV-265 instrument. Circular dichroisms (CD) were measured on a JASCO J-720 W spectropolarimeter. Enantiomeric excesses were determined by HPLC analysis (Daicel Chiralcel OD).

N-(2-*t*-butylphenyl)acetamide, (*RS*)-*N*-benzoyl-*N*-(2-*t*-butylphenyl)acetamide [(±)-**2d**] and (*RS*)-*N*-(2-*t*-butylphenyl)-*N*-(4-trifluoromethylbenzoyl)acetamide [(±)-**2g**] were prepared according to our published procedure.[4b] All reagents were available from commercial sources and used without further purification. In general, all reactions were performed in dry solvents under an argon atmosphere. All racemization experiments were performed on Taitec Thermo Minder SM-05 or Toyo Lab Thermo LH-1000. Benzene was distilled under an argon atmosphere from Na. Pyridine was distilled under an argon atmosphere from CaH_2. THF was distilled under an argon atmosphere from Na/benzophenone ketyl. Silica gel

column chromatography was performed on Kanto Chemical Silica gel 60 (spherical, 100–210 μm).

4.2. General procedure for preparation of *N*-aroyl-*N*-(2-*t*-butylphenyl)acetamides 2a–c, 2e and 2f

Method A: To a stirred solution of *N*-(2-*t*-butylphenyl)-acetamide in pyridine (0.3 M solution of the starting material) was added aroyl chloride (2.0 equiv) at 0°C. The reaction mixture was stirred at 25°C for 13 h, quenched by the addition of H_2O at 0°C and extracted with EtOAc. The organic extracts were washed with saturated aq. $NaHCO_3$ and brine, dried (Na_2SO_4) and concentrated. Purification by silica gel column afforded the analytically pure imide **2**. Recrystallization was performed with benzene–hexane as a solvent unless otherwise stated.

Method B: To a stirred solution of $ArCO_2H$ (2.0 equiv) in CH_2Cl_2 (0.3 M solution of the starting material) were added CCl_4 (12 equiv) and PPh_3 (3 equiv) at 0°C. The mixture was stirred at 25°C for 2.5 h. To this mixture were then added pyridine (10 equiv) and *N*-(2-*t*-butylphenyl)acetamide at 0°C. The whole mixture was stirred at 25°C for 12 h. The work-up was performed in the same manner as for Method A.

4.2.1. (*RS*)-*N*-(2-*t*-Butylphenyl)-*N*-(4-dimethylaminobenzoyl)acetamide [(±)-2a]. Method B was used with *N*-(2-*tert*-butylphenyl)acetamide (1.00 g, 5.23 mmol). Purification by silica gel column (EtOAc:hexane=1:3, the silica gel was pretreated with 1% Et_3N in hexane) afforded the analytically pure (±)-**2a** (666 mg, 38%) as a colorless solid along with the starting material (278 mg, 28%). Further purification of (±)-**2a** by recrystallization (benzene–hexane) afforded colorless prisms of mp 95–97°C. *Rf* value=0.32 (EtOAc:hexane=1:2). UV (MeCN): λ_{max} 340 (ϵ_{max} 25113), 235 (10832) nm. IR (nujol): ν=1702, 1661 cm^{-1}. ^1H NMR (C_6D_6): δ=1.41 (s, 9H), 2.06 (s, 3H), 2.30 (s, 6H), 6.29 (d, *J*=9.0 Hz, 2H), 6.96–7.02 (m, 3H), 7.34 (dd, *J*=8.0, 1.6 Hz, ^1H), 7.34 (d, *J*=9.0 Hz, 2H). ^{13}C NMR (C_6D_6): δ=26.44, 31.69, 36.02, 39.20, 110.52, 122.69, 126.69, 128.27, 129.04, 132.13, 133.05, 138.69, 146.94, 152.40, 171.91, 173.28. EI MS: *m/z* =338 (M^+), 279, 204, 189, 148 (bp). Anal. Calcd for $C_{21}H_{26}N_2O_2$: C, 74.52; H, 7.74; N, 8.28. Found: C, 74.69; H, 7.85; N, 8.21.

4.2.2. (*RS*)-*N*-(2-*t*-Butylphenyl)-*N*-(4-methoxybenzoyl)acetamide [(±)-2b]. Method A was used with *N*-(2-*tert*-butylphenyl)acetamide (498 mg, 2.60 mmol). Purification by silica gel column (benzene:hexane=2:1, the silica gel was pretreated with 1% Et_3N in hexane) afforded the analytically pure (±)-**2b** (703 mg, 83%) as a colorless solid. Further purification of (±)-**2b** by recrystallization (benzene) afforded colorless prisms of mp 128–129°C. *Rf* value=0.75 (EtOAc:hexane=1:2). UV (MeCN): λ_{max} 281 (ϵ_{max} 12138), 215 (22128) nm. IR (nujol): ν=1698, 1670 cm^{-1}. ^1H NMR (C_6D_6): δ=1.33 (s, 9H), 1.94 (s, 3H), 3.14 (s, 3H), 6.62 (br d, *J*=8.8 Hz, 2H), 6.87 (dd, *J*=7.7, 1.6 Hz, ^1H), 6.93 (ddd, *J*=7.7, 7.7, 1.6 Hz, ^1H), 7.04 (ddd, *J*=8.2, 7.7, 1.6 Hz, ^1H), 7.31 (dd, *J*=8.2, 1.6 Hz, ^1H), 7.80 (br d, *J*=8.8 Hz, 2H). ^{13}C NMR (C_6D_6): δ=26.23, 31.66, 35.97, 54.65, 113.30, 126.83, 128.44, 128.53, 129.16, 131.64, 132.77, 138.05, 146.86, 162.33, 171.89, 173.09. EI MS: *m/z* =325 (M^+), 266, 226, 173, 83 (bp). Anal. Calcd for $C_{20}H_{23}NO_3$: C, 73.82; H, 7.12; N, 4.30. Found: C, 73.73; H, 7.22; N, 4.31.

4.2.3. (*RS*)-*N*-(2-*t*-Butylphenyl)-*N*-(4-tolyl)acetamide [(±)-2c]. Method B was used with *N*-(2-*tert*-butylphenyl)acetamide (100 mg, 0.523 mmol). Purification by silica gel column (benzene:hexane=2:1, the silica gel was pretreated with 1% Et_3N in hexane) afforded the analytically pure (±)-**2c** (120 mg, 74%) as a colorless solid. Further purification of (±)-**2c** by recrystallization (benzene) afforded colorless prisms of mp 115–117°C. *Rf* value=0.52 (EtOAc:hexane =1:2). UV (MeCN): λ_{max} 253 (ϵ_{max} 11572), 248 (ϵ_{max} 11943), 243 (ϵ_{max} 12005) nm. IR (nujol): ν=1683 cm^{-1}. ^1H NMR (C_6D_6): δ=1.32 (s, 9H), 1.92 (s, 3H), 1.95 (s, 3H), 6.83 (dd, *J*=7.8, 1.5 Hz, ^1H), 6.87 (d, *J*=7.8 Hz, 2H), 6.91 (ddd, *J*=7.8, 7.8, 1.5 Hz, ^1H), 7.03 (ddd, *J*=7.8, 7.8, 1.5 Hz, ^1H), 7.29 (dd, *J*=7.8, 1.5 Hz, ^1H), 7.71 (d, *J*=7.8 Hz, 2H). ^{13}C NMR (C_6D_6): δ=21.48, 26.41, 31.58, 35.90, 126.87, 128.47, 128.58, 128.77, 129.15, 131.90, 132.77, 136.94, 141.89, 146.49, 172.52, 173.69. EI MS: *m/z* =309 (M^+), 267, 174, 84 (bp). Anal. Calcd for $C_{20}H_{23}NO_2$: C, 77.64; H, 7.49; N, 4.53 Found: C, 77.54; H, 7.70; N, 4.43.

4.2.4. (*RS*)-*N*-Benzoyl-*N*-(2-*t*-butylphenyl)acetamide [(±)-2d]. The physical data shown below were identical with those of our report.[4b] Colorless prisms, mp 83–84°C. UV (MeCN): λ_{max} 224 (ϵ_{max} 7383) nm. IR (KBr): ν=1687 cm^{-1}. ^1H NMR (C_6D_6): δ=1.30 (s, 9H), 1.86 (s, 3H), 6.79 (dd, *J*=7.3, 1.5 Hz, ^1H), 6.90 (ddd, *J*=7.3, 7.3, 1.5 Hz, ^1H), 7.00–7.05 (m, 4H), 7.28 (dd, *J*=7.3, 1.5 Hz, ^1H), 7.71–7.74 (m, 2H). ^{13}C NMR (C_6D_6): δ=26.15, 31.77, 36.06, 127.2, 128.1, 129.0, 129.2, 129.6, 131.3, 132.8, 136.9, 137.9, 147.3, 173.1, EI MS: *m/z*=295 (M^+), 253, 239, 149, 77 (bp).

4.2.5. (*RS*)-*N*-(2-*t*-Butylphenyl)-*N*-(4-fluorobenzoyl)-acetamide [(±)-2e]. Method A was used with *N*-(2-*tert*-butylphenyl)acetamide (510 mg, 2.67 mmol). Purification by silica gel column (EtOAc:hexane=1:8, the silica gel was pretreated with 1% Et_3N in hexane) afforded the analytically pure (±)-**2e** (827 mg, 99%) as a colorless solid. Further purification of (±)-**2e** by recrystallization (benzene–hexane) afforded colorless prisms of mp 117–120°C. *Rf* value=0.61 (EtOAc:hexane=1:2). UV (MeCN): λ_{max} 225 (ϵ_{max} 12221) nm. IR (nujol): ν=1686 cm^{-1}. ^1H NMR (C_6D_6): δ=1.27 (s, 9H), 1.82 (s, 3H), 6.66 (dd, *J*=8.5, 8.5 Hz, 2H), 6.74 (dd, *J*=7.8, 1.5 Hz, ^1H), 6.90 (ddd, *J*=7.8, 7.8, 1.5 Hz, ^1H), 7.03 (ddd, *J*=7.8, 7.8, 1.5 Hz, ^1H), 7.28 (dd, *J*=7.8, 1.5 Hz,^1H), 7.57 (dd, *J*=8.5, 5.4 Hz, 2H). ^{13}C NMR (C_6D_6): δ=26.00, 31.64, 35.94, 114.92 (d, *J*=23 Hz), 126.95, 128.76, 129.30, 131.38 (d, *J*=8.3 Hz), 132.43, 132.51 (d, *J*=3.3 Hz), 137.47, 146.81, 164.37 (d, *J*=252 Hz), 171.38, 172.83. EI MS: *m/z* =313 (M+), 254 (bp), 214, 158, 43. Anal. Calcd for $C_{19}H_{20}NO_2F$: C, 72.82; H, 6.43; N, 4.47 Found: C, 73.10; H, 6.59; N, 4.51.

4.2.6. (*RS*)-*N*-(2-*t*-Butylphenyl)-*N*-(4-chlorobenzoyl)-acetamide [(±)-2f]. Method A was used with *N*-(2-*tert*-butylphenyl)acetamide (100 mg, 0.523 mmol). Purification by silica gel column (benzene:hexane=2:1, the silica gel was pretreated with 1% Et_3N in hexane) afforded the analytically pure (±)-**2f** (171 mg, 99%) as a colorless

solid. Further purification of (±)-**2f** by recrystallization (benzene–hexane) afforded colorless prisms of mp 148–149°C. *Rf* value=0.60 (EtOAc:hexane=1:2). UV (MeCN): λ_{max} 232 (ϵ_{max} 13538) nm. IR (nujol): ν=1719, 1676 cm^{-1}. ^1H NMR (C_6D_6): δ=1.26 (s, 9H), 1.80 (s, 3H), 6.71 (dd, *J*=7.8, 1.5 Hz, ^1H), 6.89 (ddd, *J*=7.8, 7.8, 1.5 Hz, ^1H), 7.00 (d, *J*=8.5 Hz, 2H), 7.02 (ddd, *J*=7.8, 7.8, 1.5 Hz, ^1H), 7.27 (dd, *J*=7.8, 1.5 Hz, ^1H), 7.47 (d, *J*=8.5 Hz, 2H). ^{13}C NMR (C_6D_6): δ=25.94, 31.65, 35.94, 126.99, 128.13, 128.83, 129.34, 130.18, 132.32, 134.85, 137.23, 137.27, 146.81, 171.48, 172.77. EI MS: *m/z*=331 (M^++2), 329 (M^+), 272, 158, 84 (bp). Anal. Calcd for $C_{19}H_{20}NO_2Cl$: C, 69.19; H, 6.11; N, 4.25 Found: C, 69.00; H, 5.90; N, 4.51.

4.2.7. (*RS*)-*N*-(2-*t*-Butylphenyl)-*N*-(4-trifluoromethylbenzoyl)acetamide [(±)-2g]. The physical data shown below were identical with those of our report.[4b] Colorless plates, mp 125–126°C. UV (MeCN): λ_{max} 224 (ϵ_{max} 16025) nm. IR (nujol): ν=1678, 1722 cm^{-1}. ^1H NMR (C_6D_6): δ=1.26 (s, 9H), 1.73 (s, 3H), 6.70 (dd, *J*=7.7, 1.5 Hz, ^1H), 6.91 (ddd, *J*=7.7, 7.7, 1.5 Hz, ^1H), 7.03 (ddd, *J*=7.7, 7.7, 1.5 Hz, ^1H), 7.25–7.29 (m, 3H), 7.53 (d, *J*=8.1 Hz, 2H). ^{13}C NMR (C_6D_6): δ=25.76, 31.65, 35.97, 124.1 (q, *J*=272 Hz), 124.9 (q, J =3.3 Hz), 127.1, 128.6, 129.0, 129.4, 132.1, 132.1 (q, *J*=32.5 Hz), 136.9, 140.0, 146.8, 171.4, 172.6. EI MS: *m/z*=363 (M^+), 265, 149, 83 (bp). Optical resolution of (±)-**2a–g**.

Optical resolutions of (±)-**2a–g** were performed by semi-preparative HPLC using a chiral phase column (Daicel Chiralcel OD: 25 cmx1 cm i.d.). IR, NMR and MS data of optically active imides **2a–g** were identical with those of the racemates. All specific rotations shown below were measured with **2a–g** in >99% ee.

4.2.8. (*S*)-*N*-(2-*t*-Butylphenyl)-*N*-(4-dimethylaminobenzoyl)acetamide [(*S*)-2a]. Retention Time (RT)=37 min (*i*-PrOH:hexane=1:10). $[\alpha]^{22}_D$=+37° (*c* 0.70, THF). CD (MeCN): λ_{ext} 340 (Δε +0.63), 272 (−0.57), 248 (+1.71), 222 (−3.02) nm. (*R*)-**2a**. RT=30 min (*i*-PrOH:hexane =1:10). $[\alpha]^{22}_D$=−38° (*c* 0.58, THF). CD (MeCN): λ_{ext} 338 (Δε −0.36), 272 (+0.94), 248 (−1.63), 222 (+2.53) nm.

4.2.9. (*S*)-*N*-(2-*t*-Butylphenyl)-*N*-(4-methoxybenzoyl)acetamide [(*S*)-2b]. RT=20 min (*i*-PrOH:hexane=1:15). $[\alpha]^{22}_D$=+5° (*c* 0.33, THF). CD (MeCN): λ_{ext} 292 (Δε +0.42), 258 (−0.59), 234 (+0.67) nm. (*R*)-**2b**. RT=32 min (*i*-PrOH:hexane=1:15). $[\alpha]^{23}_D$=−6° (*c* 0.37, THF). CD (MeCN): λ_{ext} 290 (Δε −0.42), 258 (+0.72), 236 (−0.54) nm.

4.2.10. (*R*)-*N*-(2-*t*-Butylphenyl)-*N*-(4-tolyl)acetamide [(*R*)-2c]. RT=44 min (*i*-PrOH:hexane=1:100). $[\alpha]^{23}_D$=+26° (*c* 0.33, THF). CD (MeCN): λ_{ext} 278 (Δε +1.68), 248 (−3.12), 228 (+2.15) nm. (*S*)-**2c**. RT=30 min (*i*-PrOH: hexane=1:100). $[\alpha]^{21}_D$=−23° (*c* 0.27, THF). CD (MeCN): λ_{ext} 278 (Δε −1.57), 248 (+3.59), 228 (−2.30) nm.

4.2.11. (*R*)-*N*-Benzoyl-*N*-(2-*t*-butylphenyl)acetamide [(*R*)-2d]. RT=40 min (*i*-PrOH:hexane=1:150). $[\alpha]^{26}_D$=+29° (*c* 1.38, benzene). CD (MeCN): λ_{ext} 275 (Δε +1.31), 240 (−2.12), 220 (+2.97) nm. (*S*)-**2d**. RT=32 min (*i*-PrOH: hexane=1:150). $[\alpha]^{26}_D$=−28° (*c* 0.45, benzene). CD (MeCN): λ_{ext} 275 (Δε −1.16), 240 (+2.33), 223 (−2.48) nm.

4.2.12. (*R*)-*N*-(2-*t*-Butylphenyl)-*N*-(4-fluorobenzoyl)acetamide [(*R*)-2e]. RT=45 min (*i*-PrOH:hexane=1:100). $[\alpha]^{23}_D$=+43° (*c* 0.41, THF). CD (MeCN): λ_{ext} 272 (Δε +0.56), 240 (−0.81), 224 (+0.49) nm. (*S*)-**2e**. RT=30 min (*i*-PrOH:hexane=1:100). $[\alpha]^{23}_D$=−45° (*c* 0.36, THF). CD (MeCN): λ_{ext} 274 (Δε −1.21), 240 (+2.78), 224 (−1.61) nm.

4.2.13. (*R*)-*N*-(2-*t*-Butylphenyl)-*N*-(4-chlorobenzoyl)acetamide [(*R*)-2f]. RT=30 min (*i*-PrOH:hexane=1:100). $[\alpha]^{23}_D$=+29° (*c* 0.30, THF). CD (MeCN): λ_{ext} 278 (Δε +1.34), 248 (−3.52), 228 (+6.10) nm. (*S*)-**2f**. RT=22 min (*i*-PrOH:hexane=1:100). $[\alpha]^{23}_D$=−29° (*c* 0.32, THF). CD (MeCN): λ_{ext} 278 (Δε −1.20), 248 (+3.36), 228 (−3.74) nm.

4.2.14. (*R*)-*N*-(2-*t*-Butylphenyl)-*N*-(4-trifluoromethylbenzoyl)acetamide [(*R*)-2g]. RT=26 min (*i*-PrOH: hexane=1:100). $[\alpha]^{24}_D$=+55° (*c* 0.30, THF). CD (MeCN): λ_{ext} 278 (Δε +1.85), 238 (−3.38), 220 (+1.70) nm. (*S*)-**2g**. RT=16 min (*i*-PrOH:hexane=1:100). $[\alpha]^{20}_D$=−55° (*c* 0.42, THF). CD (MeCN): λ_{ext} 278 (Δε −1.58), 238 (+3.56), 216 (−1.10) nm.

4.3. General procedure for racemization experiment of optically active imides 2a–g

A solution of optically active imides **2a–g** (8.89×10^{-3} mmol) in benzene (3.0 mL) was stirred at each temperature (sealed-tube experiments). The rate constants shown below for their racemization were measured in the 15–70% range of reaction conversion.

2a: $10^{-6}k_{33°C}$=3.69±0.02 s^{-1}, $10^{-6}k_{40°C}$=9.08±0.02 s^{-1}, $10^{-6}k_{47°C}$=18.85±0.54 s^{-1}, $10^{-6}k_{54°C}$=44.46±1.01 s^{-1}.

2b: $10^{-6}k_{33°C}$=1.74±0.02 s^{-1}, $10^{-6}k_{40°C}$=4.26±0.37 s^{-1}, $10^{-6}k_{47°C}$=11.75±1.14 s^{-1}, $10^{-6}k_{54°C}$=25.50±0.73 s^{-1}.

2c: $10^{-6}k_{33°C}$=1.18±0.02 s^{-1}, $10^{-6}k_{40°C}$=2.93±0.02 s^{-1}, $10^{-6}k_{47°C}$=6.67±0.06 s^{-1}, $10^{-6}k_{54°C}$=16.31±0.22 s^{-1}.

2d: $10^{-6}k_{33°C}$=1.02±0.02 s^{-1}, $10^{-6}k_{40°C}$=2.73±0.09 s^{-1}, $10^{-6}k_{54°C}$=10.85±0.23 s^{-1}, $10^{-6}k_{58°C}$=24.95±0.44 s^{-1}.

2e: $10^{-6}k_{40°C}$=2.23±0.05 s^{-1}, $10^{-6}k_{47°C}$=5.76±0.05 s^{-1}, $10^{-6}k_{54°C}$=11.26±0.32 s^{-1}, $10^{-6}k_{61°C}$=27.78±0.37 s^{-1}.

2f: $10^{-6}k_{40°C}$=1.79±0.03 s^{-1}, $10^{-6}k_{47°C}$=4.51±0.07 s^{-1}, $10^{-6}k_{54°C}$=10.94±0.17 s^{-1}, $10^{-6}k_{61°C}$=26.48±0.11 s^{-1}.

2g: $10^{-6}k_{40°C}$=1.33±0.27 s^{-1}, $10^{-6}k_{47°C}$=4.10±0.07 s^{-1}, $10^{-6}k_{54°C}$=10.95±0.15 s^{-1}, $10^{-6}k_{61°C}$=24.50±0.55 s^{-1}.

4.4. (S_a,2*S*)-*N*-(2-*t*-Butylphenyl)-*N*-(4-trifluoromethylbenzoyl)-2-acetoxypropionamide (4a) and (R_a,2*S*)-*N*-(2-*t*-butylphenyl)-*N*-(4-trifluoromethylbenzoyl)-2-acetoxypropionamide (4b)

To a stirred solution of 2-*t*-butylaniline (0.92 mL, 5.90

mmol) in pyridine (14.7 mL) was added (*S*)-2-acetoxypropionyl chloride (1.5 mL, 11.8 mmol) at 0°C. The reaction mixture was stirred at 25°C for 3 h, quenched by the addition of H_2O at 0°C and extracted with EtOAc. The organic extracts were washed with saturated aq. $NaHCO_3$ and brine, dried (Na_2SO_4) and concentrated. Purification by silica gel column (EtOAc:hexane=1:10, the silica gel was pretreated with 3% Et_3N in hexane) afforded analytically pure (2*S*)-*N*-(2-*t*-butylphenyl)-2-acetoxypropionamide (**3**) (1.42 g, 91%) as a colorless solid. Recrystallization (benzene–hexane) afforded colorless prisms of mp 115–115.5°C. $[\alpha]^{20}_D=-31°$ (*c* 2.16, $CHCl_3$). *Rf* value=0.37 (EtOAc:hexane=1:2). IR (KBr): ν=3321, 1748, 1642 cm^{-1}. ^1H NMR (C_6D_6): δ=1.20 (s, 9H), 1.44 (d, *J*=6.8 Hz. 3H), 1.59 (s, 3H), 5.37 (q, *J*=6.8 Hz, ^1H), 6.98 (ddd, *J*=8.1, 8.1, 1.5 Hz ^1H), 7.12 (ddd, *J*=8.1, 8.1, 1.5 Hz, ^1H), 7.23 (dd, *J*=8.1, 1.5 Hz, ^1H), 7.91 (br s, 1 H), 8.30 (br d *J*=8.1 Hz, ^1H). ^{13}C NMR (C_6D_6): δ=17.77, 20.35, 30.36, 34.24, 71.21, 125.40, 126.09, 126.25, 126.91, 135.38, 140.39, 167.19, 168.00. EI MS: *m/z*=263 (M^+), 206, 132, 88 (bp). Anal. Calcd for $C_{15}H_{21}NO_3$: C, 68.42; H, 8.04; N, 5.32. Found: C, 68.56; H, 8.04; N, 5.25. To a stirred solution of (2*S*)-*N*-(2-*t*-butylphenyl)-2-acetoxypropionamide (**3**) (20.3 mg, 0.08 mmol) in pyridine (0.3 mL) was added 4-trifluoromethylbenzoyl chloride (0.07 mL, 0.47 mmol) at 0°C. The reaction mixture was stirred at 25°C for 16 h, quenched by the addition of H_2O at 0°C and extracted with EtOAc. The organic extracts were washed with saturated aq. $NaHCO_3$ and brine, dried (Na_2SO_4) and concentrated. Purification by silica gel column (EtOAc:hexane=1:10, the silica gel was pretreated with 3% Et_3N in hexane) afforded the analytically pure **4a** (21.2 mg, 63%, 99% ee) and **4b** (11.0 mg, 33%, 91% ee) as colorless solids. **4a**: Colorless prisms, mp 95–96.5°C (hexane, 98% ee). $[\alpha]^{20}_D=-258°$ (*c* 2.72, benzene, 98% ee), *Rf* value=0.61 (EtOAc:hexane=1:2). IR (nujol): ν=1738, 1712, 1684 cm^{-1}. ^1H NMR (C_6D_6): δ=1.21 (s, 9H), 1.65 (s, 3H), 1.71 (d, *J*=6.6 Hz, 3H), 5.74 (q, *J*=6.6 Hz, ^1H) 6.82–6.89 (m, 2H), 7.03 (d, *J*=8.3 Hz, 2H), 7.06–7.09 (m, ^1H), 7.46–7.49 (m, 3H). ^{13}C NMR ($CDCl_3$): δ=16.58, 20.56, 31.86, 36.11, 71.11, 123.11 (q, *J*=272 Hz), 124.54 (q, *J*=3.3 Hz), 126.63, 129.05, 129.20, 129.59, 132.34 (q, *J*=33 Hz), 132.54, 134.66, 138.14, 147.63, 170.75, 171.23, 175.21. EI MS: *m/z*=435 (M+), 374, 263, 173 (bp). Anal. Calcd for $C_{23}H_{24}NO_4F_3$: C, 63.44; H, 5.56; N, 3.22. Found: C, 63.72; H, 5.65; N, 3.19. **4b**: Colorless prisms, mp 124–125°C (benzene–hexane, 94% ee). $[\alpha]^{24}_D=-86°$ (*c* 1.02, benzene, 94% ee). *Rf* value=0.56 (EtOAc:hexane =1:2). IR (nujol): ν=1733, 1673 cm^{-1}. ^1H NMR (C_6D_6): δ=1.29 (d, *J*=6.6 Hz, 3H), 1.30 (s, 9H), 1.65 (s, 3H), 5.70 (q, *J*=6.6 Hz, ^1H), 6.88 (ddd, *J*=7.6, 7.6, 1.7 Hz, ^1H), 6.97–7.05 (m, 2H), 7.21 (d, *J*=8.3 Hz, 2H), 7.25 (dd, *J*=7.6, 1.7 Hz, ^1H), 7.51 (d, *J*=8.3 Hz, 2H). ^{13}C NMR (C_6D_6): δ=16.30, 20.13, 32.16, 36.54, 70.16, 123.95 (q, *J*=272 Hz), 124.83 (q, *J*=4.2 Hz), 126.77, 129.33, 130.37, 132.01, 132.19 (q, *J*=32.5 Hz), 134.87, 139.40, 148.28, 169.17, 171.03, 173.53. EI MS: *m/z*=435 (M+), 291, 248, 134 (bp). Anal. Calcd for $C_{23}H_{24}NO_4F_3$: C, 63.44; H, 5.56; N, 3.22. Found: C, 63.74; H, 5.43; N, 3.16.

4.4.1. (*R*)-*N*-(2-*t*-butylphenyl)-*N*-(4-trifluoromethylbenzoyl)propionamide (5a). To a stirred solution of **4a** (24.2 mg, 0.056 mmol, 99% ee) in THF (0.2 mL) was added SmI_2, 0.1 M solution in THF (1.7 mL, 0.170 mmol) at −44°C. The reaction mixture was stirred at −44°C for 20 min, and quenched by the addition of hexane and silica gel at the same temperature. The whole mixture was filtered to remove the silica gel and concentrated. Purification by silica gel column (EtOAc:hexane=1:10, the silica gel was pretreated with 3% Et_3N in hexane) afforded **5a** (20.1 mg, 95%, 97% ee) as a colorless solid. Recrystallization (benzene–hexane) afforded colorless prisms of mp 124.5–125°C (71% ee). *Rf* value=0.68 (EtOAc:hexane =1:2). UV (MeCN): λ_{max} 224 (ϵ_{max} 17569) nm. CD (MeCN): λ_{ext} 281 (+1.18), 239 (−2.27), 224 (+7.19) nm. $[\alpha]^{20}_D=+87°$ (*c* 1.08, THF, 71% ee). IR (nujol): ν=1721, 1678 cm^{-1}. ^1H NMR (C_6D_6): δ=0.89 (t, *J*=7.3 Hz, 3H), 1.28 (s, 9H), 1.97–2.05 (m, 2H), 6.73 (dd, *J*=7.8, 1.7 Hz, ^1H), 6.94 (ddd, *J*=7.8, 7.8, 1.7 Hz, ^1H), 7.06 (ddd, *J*=7.8, 7.8, 1.7 Hz, ^1H), 7.28 (d, *J*=8.1 Hz, 2H), 7.31 (dd, *J*=7.8, 1.7 Hz, ^1H), 7.52 (d, *J*=8.1 Hz, 2H). ^{13}C NMR (C_6D_6): δ=8.85, 31.45, 31.72, 36.07, 124.13 (q, *J*=272 Hz), 124.92 (q, *J*=3.3 Hz), 127.12, 128.36, 129.04, 129.51, 132.05 (q, *J*=32.5 Hz), 132.09, 136.68, 140.30, 147.10, 171.48, 176.22. EI MS: *m/z*=377 (M^+), 320, 264, 132 (bp). Anal. Calcd for $C_{21}H_{22}NO_2F_3$: C, 66.83; H, 5.88; N, 3.71. Found: C, 67.18; H, 5.98; N, 3.86.

4.4.2. (*S*)-*N*-(2-*t*-butylphenyl)-*N*-(4-trifluoromethylbenzoyl)propionamide (5b). The same manner for the synthesis of **5a** was used with **4b** (91%ee) to afford **5b** (81%, 90% ee). Colorless prisms (benzene–hexane), mp 123–124°C (90% ee). $[\alpha]^{20}_D=-110°$ (*c* 1.06, THF, 90% ee). CD (MeCN): λ_{ext} 280 (−1.01), 238 (+2.72), 222 (−4.15) nm. Other spectral data of **5b** were identical with those of **5a**.

Crystal data and refinement for **2a** and **4b**.

2a: $C_{21}H_{26}N_2O_2$, *M*=338.45, monoclinic, a=19.654(3) Å *b*=8.307(2) Å *c*=12.142(3) Å β=99.77(2)°, *V*=1953.7(7) $Å^3$, space group $P2_1/c$ (# 14), *Z*=4, D_{calc}=1.151 g cm^{-3}. Crystal dimensions 0.40×0.40×0.15 mm, μ(CuKα)=5.86 cm^{-1}. Data collection and processing: AFC7S diffractometer, graphite monochromated MoKα (λ=1.54178 Å) radiation, 4018 reflections measured, giving 2158 with $I>3.00\sigma$ (*I*). The structure was solved by direct methods using SIR92[16a] and was refined by full-matrix least-squares techniques using DIRDIF94.[17] The non-hydrogen atoms were refined anisotropically. The final residuals for reflections with $I>3.00\sigma$ (*I*) were *R*=0.088, *Rw*=0.075. Full details of the crystallographic results have been deposited with the Cambridge Crystallographic Data Center (no. CCDC 160500).

4b: $C_{23}H_{24}NO_4F_3$, *M*=435.44, orthorhombic, *a*=9.021(1) Å, *b*=9.386(1) Å, *c*=25.868(4) Å, *V*=2190.2(5) $Å^3$, space group $P2_12_12_1$ (# 19), *Z*=4, D_{calc}=1.320 g cm^{-3}. Crystal dimensions 0.50×0.45×0.45 mm, μ(MoKα)=1.06 cm^{-1}. Data collection and processing: CCD diffractometer, graphite monochromated MoKα (λ=0.71069 Å) radiation, 12744 reflections measured, giving 2735 with $I>0.50\sigma$ (*I*). The structure was solved by direct methods using SIR97[16b] and was refined by full-matrix least-squares techniques using DIRDIF94.[17] The non-hydrogen atoms were refined anisotropically. The final residuals for reflections with

$I>0.50\sigma$ (I) were $R=0.041$, $Rw=0.044$. Full details of the crystallographic results have been deposited with the Cambridge Crystallographic Data Center (no. CCDC 160501).

Acknowledgements

We thank the Ministry of Education, Science and Culture, Japan for support. K. K. was financially supported by the Mitsubishi Chemical Corporation Fund and the Uehara Memorial Foundation.

References

1. Reports for a cyclic imide and an amide N–Ar axis: (a) Curran, D. P.; Qi, H.; Geib, S. J.; DeMello, N. C. *J. Am. Chem. Soc.* **1994**, *116*, 3131–3132. (b) Azumaya, I.; Yamaguchi, K.; Okamoto, I.; Kagechika, H.; Shudo, K. *J. Am. Chem. Soc.* **1995**, *117*, 9083–9084. (c) Hughes, A. D.; Price, D. A.; Shishkin, O.; Simpkins, N. S. *Tetrahedron Lett.* **1996**, *37*, 7607–7610. (d) Kitagawa, O.; Izawa, H.; Taguchi, T.; Shiro, M. *Tetrahedron Lett.* **1997**, *38*, 4447–4450. (e) Curran, D. P.; Hale, G. R.; Geib, S. J.; Balog, A.; Cass, Q. B.; Degani, A. L. G.; Hernandes, M. Z.; Freita, L. C. G. *Tetrahedron: Asymmetry* **1997**, *8*, 3955–3975. (f) Kitagawa, O.; Izawa, H.; Sato, K.; Dobashi, A.; Taguchi, T.; Shiro, M. *J. Org. Chem.* **1998**, *63*, 2634–2640. (g) Clayden, J. *Synlett* **1998**, 810–816. (h) Hughes, A. D.; Simpkins, N. S. *Synlett* **1998**, 967–968. (i) Fujita, M.; Kitagawa, O.; Izawa, H.; Dobashi, A.; Fukaya, H.; Taguchi, T. *Tetrahedron Lett.* **1999**, *40*, 1949–1952. (j) Hughes, A. D.; Price, D. A.; Simpkins, N. S. *J. Chem. Soc., Perkin Trans 1* **1999**, 1295–1304. (k) Kitagawa, O.; Momose, S.; Fushimi, Y.; Taguchi, T. *Tetrahedron Lett.* **1999**, *40*, 8827–8831. (l) Curran, D. P.; Liu, W.; Chen, C. H. *J. Am. Chem. Soc.* **1999**, *121*, 11012–11013. (m) Godfrey, C. R. A.; Simpkins, N. S.; Walker, M. D. *Synlett* **2000**, 388–390. (n) Fujita, M.; Kitagawa, O.; Yamada, Y.; Izawa, H.; Hasegawa, H.; Taguchi, T. *J. Org. Chem.* **2000**, *65*, 1108–1114. (o) Shimizu, K. D.; Heather, O. F.; Richard, D. A. *Tetrahedron Lett.* **2000**, *41*, 5431–5434. (p) Kawabata, T.; Suzuki, H.; Nagase, Y.; Fuji, K. *Angew. Chem. Int. Ed.* **2000**, *39*, 2155–2157. (q) Kitagawa, O.; Fujita, M.; Kohriyama, M.; Hasegawa, H.; Taguchi, T. *Tetrahedron Lett.* **2000**, *41*, 8539–8544.
2. For recent reports in relation to non-biaryl axial chirality except an N–Ar axis, see: (a) Kawabata, T.; Yahiro, K.; Fuji, K. *J. Am. Chem. Soc.* **1991**, *113*, 9694–9696. (b) Dogan, I.; Pustet, N.; Mannschreck, A. *J. Chem. Soc., Perkin Trans. 2* **1993**, 1557–1560. (c) Ohno, A.; Kunitomo, J.; Kawai, Y.; Kawamoto, T.; Tomishima, M.; Yoneda, F. *J. Org. Chem.* **1996**, *61*, 9344–9355. (d) Ikeura, Y.; Ishichi, Y.; Tanaka, T.; Fujishima, A.; Murabayashi, M.; Kawada, M.; Ishimaru, T.; Kamo, I.; Doi, T.; Natsugari, H. *J. Med. Chem.* **1998**, *41*, 4232–4239. (e) Koide, H.; Uemura, M. *Chirality* **2000**, *12*, 352–359.
3. For recent studies in relation to the rotational barrier around a cyclic imide N–Ar bond, see: (a) Kishikawa, K.; Tsuru, I.; Kohmoto, S.; Yamamoto, M.; Yamada, K. *Chem. Lett.* **1994**, 1605–1606. (b) Kishikawa, K.; Yoshizaki, K.; Kohmoto, S.; Yamamoto, M.; Yamaguchi, K.; Yamada, K. *J. Chem. Soc., Perkin Trans. 1* **1997**, 1233–1239.
4. (a) Kondo, K.; Fujita, H.; Suzuki, T.; Murakami, Y. *Tetrahedron Lett.* **1999**, *40*, 5577–5580. (b) Kondo, K.; Iida, T.; Fujita, H.; Suzuki, T.; Yamaguchi, K.; Murakami, Y. *Tetrahedron* **2000**, *56*, 8883–8891.
5. For our preliminary communication on the electronic effects of acyl groups, see: Kondo, K.; Fujita, H.; Suzuki, T.; Murakami, Y. *Enantiomer* **2000**, *5*, 115–118.
6. According to Eyring's equation, $\Delta H^{\ddagger}$ and $\Delta S^{\ddagger}$ of **2a–g** were calculated. For Eyring's equation, see: Cagle, Jr., F. W.; Eyring, H. *J. Am. Chem. Soc.* **1951**, *73*, 5628–5630.
7. Hammett, L. P. *Physical Organic Chemistry*, 2nd ed.; McGraw-Hill: New York, 1970.
8. In the case of a simple acyclic imide, the *endo–exo* arrangement of imide carbonyl groups would be the generally preferred conformation, see: Noe, E. A.; Raban, M. *J. Am. Chem. Soc.* **1975**, *97*, 5811–5820.
9. (a) Winkler, F. K.; Dunitz, J. D. *J. Mol. Biol.* **1971**, *59*, 169–182. (b) Dunitz, J. D.; Winkler, F. K. *Acta. Cryst.* **1975**, *B31*, 251–263.
10. Twist angle τ is defined as follows: $\tau=1/2\ (\omega_1+\omega_2)$. According to the definition, the τ value lies in the range between $-180°$ and $180°$. However, the larger the distortion, the nearer the value lies to $90°$ or $-90°$; on the other hand, the smaller the distortion, the nearer the value lies to $0°$, $180°$, or $-180°$. Therefore, in order to avoid confusion regarding the magnitude of τ, we represented the twist angle as $|\tau|$ (for $0°\leq|\tau|\leq90°$) or 180-$|\tau|$ (for $90°\leq|\tau|$), see: Yamada, S. *Angew. Chem. Int. Ed. Engl.* **1993**, *32*, 1083–1085.
11. Yamada, S.; Nunami, N.; Hori, K. *Chem. Lett.* **1998**, 451–452.
12. No marked change in the imide moiety between *N*-(4-*t*-butylphenyl)-*N*-(4-dimethylaminobenzoyl)acetamide and *N*-(4-*t*-butylphenyl)-*N*-(4-trifluoromethylbenzoyl)acetamide was observed by X-ray analysis. For a recent report of pyramidal amide nitrogen, see: Ohwada, T.; Achiwa, T.; Okamoto, I.; Shudo, K.; Yamaguchi, K. *Tetrahedron Lett.* **1998**, *39*, 865–868.
13. The imide geometry of **5b** was considered to be the *exo–endo* arrangement with acetyl carbonyl *trans* and aroyl carbonyl *cis* to the 2-*t*-butylphenyl group, although that of **4b** was the *endo–exo* arrangement as shown in Fig. 3. In fact, the CD Cotton effect of **4b** was not observed.
14. For the CD exciton chirality method, see: Harada, N., Nakanishi, K. Circular Dichroic Spectroscopy–Exciton Coupling in Organic Chemistry; University Science Books: Mill Valley, 1983.
15. (a) For a pioneering report of deacetoxylation with SmI_2, see: Molander, G.A., Hahn, G. *J. Org. Chem.* **1986**, *51*, 1135–1138. (b) Quite recently, similar asymmetric synthesis of anilides has been reported by Simpkins et al., see Ref. 1(j).
16. (a) Altomare, A.; Cascarano, M.; Giacovazzo, C.; Guagliardi, A. *J. Appl. Cryst.* **1993**, *26*, 343–350. (b) Altomare, A.; Burla, M. C.; Camalli, M.; Cascarano, G. L.; Giacovazzo, C.; Guagliardi, A.; Moliterni, A. G. G.; Polidori, G.; Spagna, R. *J. Appl. Cryst.* **1999**, *32*, 115–119.
17. Beurskens, P. T.; Admiraal, G.; Beurskens, G.; Bosman, W. P.; de Gelder, R.; Israel, R.; Smits, J. M. M.; the DIRDIF-94 program system, Technical Report of the Crystallography Laboratory, University of Nijmegen, The Netherlands, 1994.